

---

## Abstract

This chapter treats the main choices, issues, and tradeoffs in the design of flapping wing MAVs. In particular, we discuss the implications of different tail and wing configurations, the energy source and various types of actuators. We also show how choices elementary to aircraft design, such as the trade-off between fuel/battery mass and payload mass can have rather large effects at the scale of light-weight flapping wing MAVs.

---

## 2.1 Introduction

The design of flapping wing MAVs is still a very active area of research. While the model plane world has known small rubber band powered ornithopters since the 1870s [4], the first electric powered flapping wing MAV, named the *MicroBat*, only flew in 1998 [28]. The design of flapping wing MAVs until now mainly progressed by means of trial-and-error. Automatic optimization is still very unreliable due to a lack of accurate theoretical models. Especially the design decisions concerning the shape, tension, and materials of the wings cannot be made purely on the basis of simulation due to a lack in knowledge on the aerodynamics around flexible airfoils.

Despite the lack of full theoretical grounding of all design choices, many functioning flapping wing designs have been made. Looking into these existing designs reveals some insights that may help to understand the key challenges and tradeoffs involved in flapping wing design. With these existing flapping wing MAV designs in mind, we discuss some of the main design choices and their consequences. We start with the general design concept in Sect. 2.2. Subsequently, the important choice of tail configuration is discussed in Sect. 2.3. This is followed by the wing configuration and single wing design (Sect. 2.4). We explain various methods to control the MAV and the possible implementations of such methods with actuators in Sect. 2.5. In Sect. 2.6 we discuss some of the choices that influence the energy and power

available to flapping wing MAVs to perform their missions. Then, we touch upon the drive mechanism used to achieve flapping wing movements of the right frequency in Sect. 2.7. Finally, we draw conclusions in Sect. 2.8.

---

## 2.2 General Design Concept

An aircraft design is highly dependent on the intended use of the platform. The driving force in the design can be to optimize for maximum endurance on one hand, or on the contrary to optimize for minimum size. Typically the goal also includes other aspects such as stability or payload capability. Different combinations of goals can lead to very different designs. Common to almost all of these goals is that they are harder to attain at smaller scales. There are coarsely two approaches to finally arrive at fully functioning fly-sized flapping wing MAVs: bottom-up and top-down.

The bottom-up approach focuses on constructing and testing the tiny parts necessary for directly constructing a fly-sized robot [25,31,32,38]. Research studies adopting this approach often tackle extremely difficult sub-tasks such as the construction of the insect thorax [39], or the generation of sufficient thrust [2]. Some of the most ground-breaking early work was performed on the Micromechanical Flying Insect (MFI) [11]. In recent work, researchers from Harvard published on the first controlled flights of their fly-sized robot named *Robobee* [25,38]. The Robobee can be fully controlled, both attitude and position, by using control of the two fly-sized wings. In [25], the control relied on an external motion tracking system. However, later studies already used onboard sensors [12,30]. While the energy for flight is currently still provided externally via wires, the plans are to integrate the energy and also processing on board the flapping wing MAV.

The top-down approach starts with relatively larger scale but fully functioning flapping wing MAVs (e.g., [7]). The idea behind the approach is that studying such MAVs can lead to insights for the construction of a following, smaller or smarter version. One advantage of this approach is that it allows interplay between theory and practice. For aerodynamics research, having a flying system ensures that the research is directed to aspects that also have a practical relevance. For artificial intelligence research, having a physical and fully functioning MAV is of great value: real-world tests force the experimenters to take into account all aspects of the robotic system. In addition, they reveal physical properties of the system that can be exploited by the algorithms.

The bottom-up and top-down approach have complementary advantages and risks. For example, a risk of the top-down approach is that the research will focus too much on incremental modifications of the MAV, ignoring possible disruptive improvements. On the other hand, a risk of the bottom-up approach is that research may focus too much on detailed aspects that might turn out irrelevant for a fully flying system. The bottom-up approach can lead to fundamental new understanding and techniques, while the practical ‘surprises’ of the top-down approach give insight

into pressing problems of lacking scientific knowledge or technology. We believe that progress in flapping wing research requires both approaches to exist.

In the DelFly project a top-down approach was adopted, because of our interest, expertise, and means. In what follows, we will mostly limit ourselves to fully functioning MAV designs, carrying their energy source on board.

---

### 2.3 Tail Configuration

Perhaps the most influential design choice of a flapping wing MAV is its tail configuration. A tail damps the rotational dynamics, implying that around the nominal flight condition the flapping wing MAV has a passively stable attitude. Since a tailed design does not necessarily need active control for stabilizing the attitude, there is no need for an onboard Inertial Measurement Unit (IMU) or autopilot. In addition, directional control can be achieved with parts of the tail, as is done with normal fixed wing aircraft (see Sect. 2.5). The wings do not have to be used for directional control and can be realized with relatively straightforward mechanisms. Figure 2.1 shows different possible tails, including a conventional plane tail (I - from [17]), inverted V-tail (II - from [7]), and a tail that also serves as a landing gear (III - from [7]).

A tailless design is closer to the anatomy of flying insects, but makes the platform's attitude passively unstable [19,33,34]. As a consequence, a high-bandwidth control system needs to act continuously in order to stabilize the attitude. How to achieve

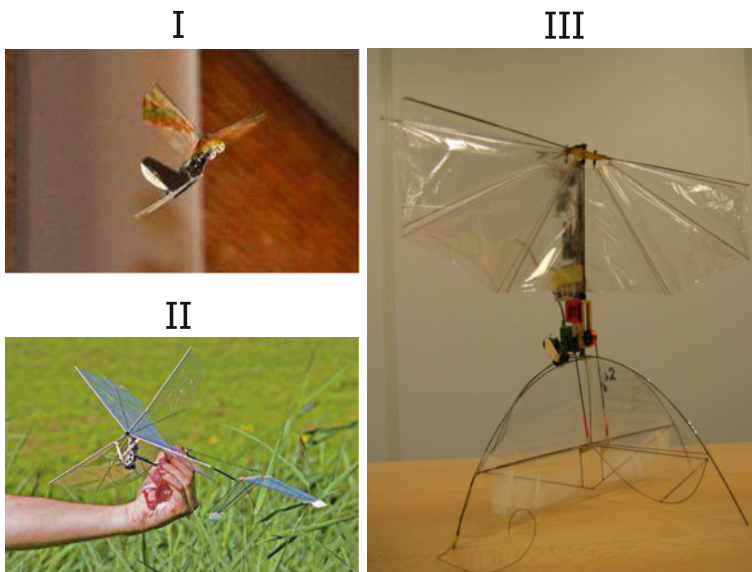


**Fig. 2.1** Different tail designs: (I) conventional plane tail, Wright State University flapping wing MAV [17], (II) inverted V-tail, DelFly I [7], and (III) ‘standing tail’, DelFly II [7]. Images reprinted with permission

**Fig. 2.2** Nano Hummingbird tailless design [20]—public domain image from [6]



this with the various degrees of freedom of flapping wings was for a long time an open question. A control system can for example change the flapping frequency of the individual wings, the phasing of their flapping cycles, the flapping amplitudes, possibly the angles of the wings during the flapping cycle, etc. There was already theoretical work on the principles that could establish attitude stabilization (e.g., [9, 10]). However, the first design actually realizing controlled flight of a tailless MAV was the Nano Hummingbird [20], shown in Fig. 2.2.

---

## 2.4 Wing Configuration and Design

Based on the tail configuration, a specific wing configuration can be chosen. Figure 2.3 shows a number of such configurations. The most ‘traditional’ designs are perhaps the ones with single wings (e.g., as in the ‘Small bird’ / ‘Big bird’ [15]). Figure 2.3 I shows the design of the ‘Robo Raven’, which can actuate its left and right wings independently of each other. Another bio-mimicking design is that with two wing pairs behind each other, as in the dragonfly (Fig. 2.3 - II) [13]. Going beyond nature, there are also designs that feature four wings with the same stroke plane (e.g., [1, 7, 17, 24, 41]) (Fig. 2.3 - IIIa/b/c). The wings of these designs typically almost touch each other at one or more points during the flapping cycle. When they do, they first ‘clap’ together and then ‘fling’ apart, providing additional lift (see Chap. 5). The wings can perform a single clap-and-fling (IIIa), a double clap-and-fling (IIIb), or multiple clap-and-flings simultaneously (IIIc) both during the outstroke and the instroke. Obviously, the wing configuration has large consequences on the forces generated by the flapping and on the way in which the MAV can be controlled.

After choosing a wing configuration, there still remain endless probabilities for designing the individual wings. The wing design is very important for the aerodynamic performance, and hence the lift that can be generated by the flapping wing

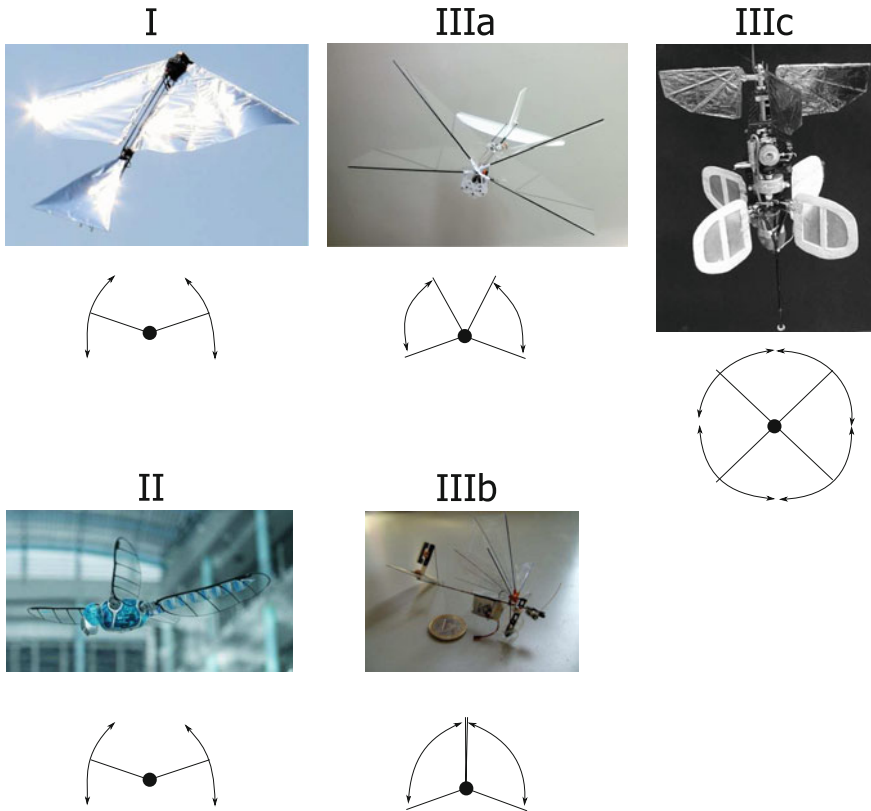


**Fig. 2.3** Different wing configurations: (I) the ‘Robo Raven’ [14], (II) dragonfly setup of the ‘Bionicopter’ [13], (IIIa) DelFly II, (IIIb) DelFly Micro with double clap-and-fling (public domain image from [37]), (IIIc) the ‘Mentor’ [41]. All images reprinted with permission

MAV. It involves a choice of the materials for the structuring elements and wing membrane, and the way to combine these to form the wing’s shape and structure.

A traditional choice for the wing materials consists of PET-foil and carbon fiber reinforced polymer (CFRP) rods. These materials have proven their worth, are widely available, and do not require specific infrastructure for construction. The downside is that they typically require some manual work, which can limit repeatability. Moreover, the design options with these materials are relatively limited. Most designs with PET-foil and rods are limited to geometric shapes with a stiff leading edge and a few stiffeners added to the wing. In order to allow for more intricate, and yet repeatable designs, other materials and fabrication methods have been investigated. For example, the early MicroBat project involved the creation of MEMS wings in various shapes [28]. In a more recent study, a complete flapping wing MAV has been 3D-printed [29]. Although these methods are very promising, they still face challenges concerning fatigue and lifetime.

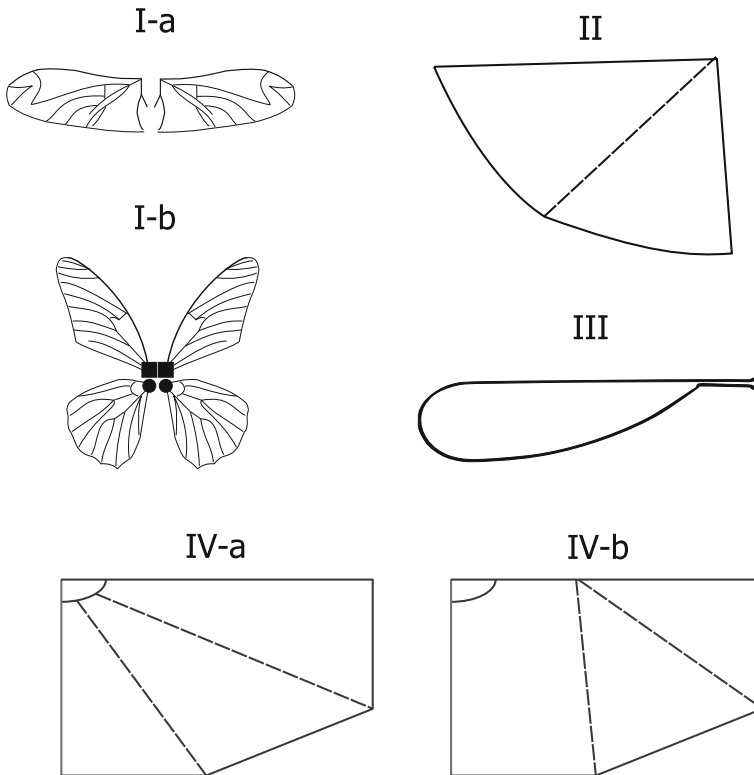


**Fig. 2.4** Different wing designs: (I-a)/(I-b) sketches of the designs tested out for the MicroBat design [28], (II) sketch of the wing design of ‘Small Bird’ [3], (III) sketch of the 3D-printed wing by [29], and (IV-a)/(IV-b) sketches of DelFly II wings [8]

Based on the selected materials and fabrication method, a wing shape can be envisaged. Figure 2.4 shows different wing shapes from a number of studies [3, 8, 28, 29]. Wing designs I-a and I-b are examples of bio-mimicking wing designs, here copying the structure of a beetle and butterfly wing, respectively. The ‘biomimicking’ wings are often not the optimal ones for flapping wing MAVs (as was also the case in [28]). Wing design II, of the FWMAV ‘Small Bird’ [3], is perhaps closest to the rubber-powered ornithopters mentioned in the introduction. It uses a ‘round’ trailing edge. Wing design III is used on the 3D-printed flapping wing MAV presented in [29]. It has a ‘round’, solid outlining. It lacks stiffeners on the inside of the wing. Wing designs IV-a and IV-b use traditional PET foil and carbon stiffeners, but they do not have the round edges in order to improve the wing’s efficiency [7]. The difference between wings IV-a and IV-b lies in the positioning of the stiffeners, leading to a significant difference in aerodynamic performance [8].

## 2.5 Control and Actuators

### 2.5.1 Actuation Strategies

Natural fliers use several strategies to control the flight. Whereas birds use their tails, flies rely mostly on their wings (and in some cases their legs). Also flapping wing MAVs can use the tail and / or the wings for control.

For tailed FWMAVs, several different actuation schemes have been devised, of which some examples are shown in the top row of Fig. 2.5. In the figure, the actuated elements are colored in orange. A common design is to have a conventional aircraft tail (design I in Fig. 2.5) with an elevator and a rudder. The elevator induces a pitching moment (see Fig. 10.2 for the definition of rotations and axes). The rudder has coupled effects. It initially induces a yaw moment, which in turn causes rolling. Design II shows a design as used on Wowwee's Flytech Dragonfly. It yaws by means of a tail rotor, just like a helicopter. Another option is to use a ruddervator, shown as design III in Fig. 2.5. This setup involves two actuated control surfaces on an inverted v-tail. The inverted v-tail has several advantages. For instance, it uses fewer tail surfaces, leading to lower interference drag and construction and weight advantages. Moreover, the tail produces a combined yawing and rolling moment that support each other. A drawback

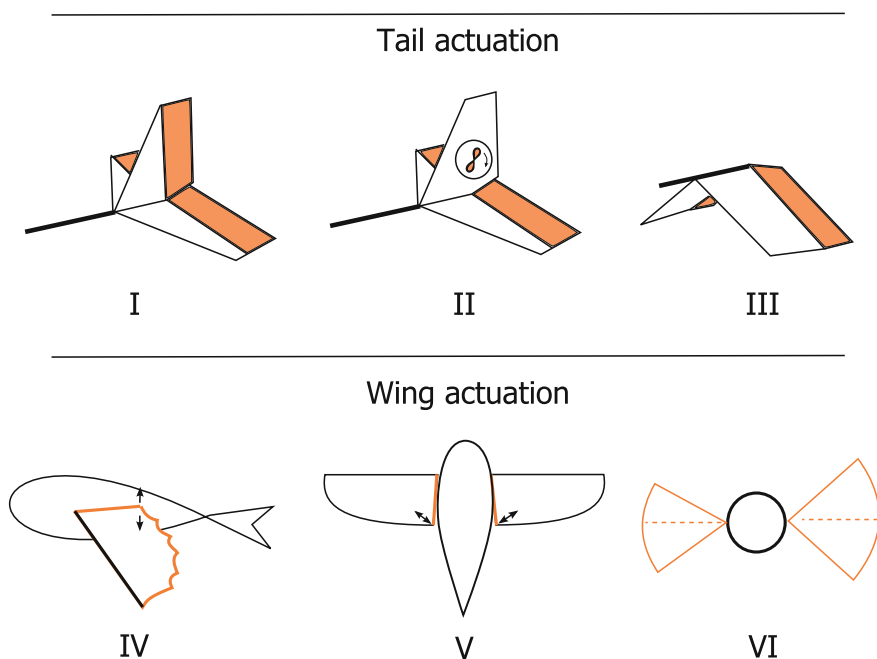


**Fig. 2.5** Various actuation methods: (I) aircraft tail, (II) aircraft tail with a propeller for yawing, (III) inverted V-tail, (IV) changing the incidence of the wings in forward flight, (V) tensioning the wings for tailless hover flight, and (VI) changing the stroke amplitude and mean stroke position

arises from the coupled effects of actuating the control surfaces. For instance, a yawing deflection reduces the maximum attainable pitching deflection. In addition, the inverted v-tail makes landings more difficult - more easily leading to damage.

In contrast to birds, insects use their wings for both propulsion and control, which provides them with significant control authority and allows for aggressive maneuvers. The actuation design IV shown in Fig. 2.5 has been designed for the Vamp / Wasp toys. Instead of using the tail, the incidence of each wing is changed to introduce a yawing action that will result in turning. In order to turn, one wing is given a higher incidence than the other. The higher incidence wing will be subject to more drag, which causes the ornithopter to yaw. In the same time, the higher incidence wing will generate more lift, which will make the ornithopter roll slightly in the opposite direction. This control for turning works reasonably well at low speeds at which the aircraft is trimmed: the ornithopter will turn in the direction of the higher incidence wing. At higher speeds the adverse yaw effect diminishes and the roll effect starts to dominate. As a consequence, the control action will reverse, with the ornithopter turning toward the lower incidence wing. Hence, this control scheme is a problem if the ornithopter has to fly at very different speeds.

The actuation scheme V in Fig. 2.5 is used on the Nano Hummingbird [20]. The bars allow to tension / relax the wings, which will increase / decrease the lift generated by the wing. If the left wing is tensioned more than the right wing, a roll moment will be created. If both wings are tensioned more during the aft part of the flap stroke (behind the MAV), then a forward pitch moment will be created. A yaw moment is created when the wings are tightened asymmetrically, for one wing during the forward motion and for the other wing during the backward motion of the flap stroke. Alternatives to this method for hovering single wing MAVs have also been investigated. In [18] the flapping amplitude and the mean position of the flapping stroke are changed (method VI in Fig. 2.5). Increasing the flapping amplitude results in an increase in lift, while changing the mean position of the flapping stroke can create a pitch or yaw moment. A similar strategy is employed in the Robobee [25].

## 2.5.2 Actuators

In order to implement a control scheme, an actuator is necessary. Various actuators that are available (shown in Fig. 2.6) will be discussed here with their relevant properties, including mass, size, force, and speed.

Magnetic actuators (Fig. 2.6, I) are pulse width modulation (PWM) driven with a duty cycle proportional to the transmitter control stick, which results in a proportional current. This current produces a moment in the magnet which again translates to a proportional force that goes to the control surface. However the force is small and with the air pressure on the control surfaces being proportional to the air velocity squared, the control throw gets much lower at higher airspeed. This can cause inability to pull up from fast descending flight.



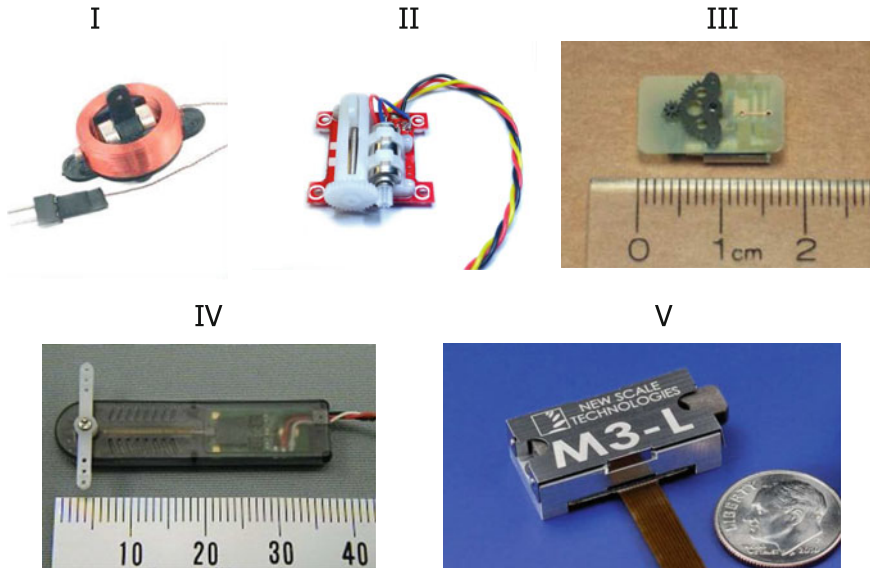


**Fig. 2.6** Various actuators: (I) magnetic actuator by Plantraco [27], (II) conventional servo by Hobby King [21], (III) conventional servo by Microflierradio [23], (IV) Muscle wire by Toki ([5]), and (V) Piezo servo by New Scale [35]. Images reprinted with permission

An alternative consists of conventional servos (Fig. 2.6, II and III) that use a small electric motor, gearing and a potentiometer or magnetic-Hall sensor for position feedback. This type of actuator has more force and a higher accuracy compared to the magnetic actuator. Two example servos are shown in Fig. 2.6. Number II is a linear servo weighting only 1.1 g; it is industrially produced and marketed by Hobby King under the name Ultra Micro. The Ultra Micro is very close to a conventional servo but designed with size and weight reduction in mind. The linear potentiometer for feedback is also used as an attachment for the mechanical output. Even lighter designs are available, such as number III in Fig. 2.6, which is a rotary servo produced by Micro Flier Radio weighing 0.45 g.

Muscle wire is another option (Fig. 2.6, IV). It contracts when it is heated and relaxes when it cools down again. This is used to actuate a pivot where two wires work in conjunction. Because the contracted / heated wire has a lower resistance, a position feedback based on the differential resistance is employed for the servo action. The initial movement from cooled condition is relatively quick, while the relaxation to the neutral position is much slower. The cooling of the wire is limiting the actuation speed. For instance, when used with the DeFly, the speed was insufficient and the wires a bit too fragile.

Finally, Piezo-based servos can be used (Fig. 2.6, V). For instance, the New Scale M3-L is currently the smallest Piezo-based servo that could be used in small UAVs. Intrinsically the piezo servo can be very light, the heart of it measures only  $2.8 \times 2.8 \times 6$  mm, but the high voltage electronics to drive the actuator and incorporate feedback

**Table 2.1** Different actuators and their properties

		Magnetic actuator	Ultra micro servo	Bio wire servo	Linear servo
Manufact.		Plantraco	Microflier	Toki	HK UM
Mass	gr	0.7	0.45	1.0	1.1
Size	mm	10 × 7	12 × 10 × 6	38 × 9 × 3	18 × 15 × 8
Force	N	0.01	0.15	0.15	0.35
Stroke	mm	± 4	± 4	± 4	± 4
Speed	sec	0.1	0.15	+0.3 –0.9	0.18
Power idle	mA	0	5	5	5
Power Avg	mA	20	30	30	30
Power max	mA	80	100	80	120
		Micro servo HS5035HD	Piezo servo M3-L	Bare piezo plus electronics	
Manufact.		HiTec	New scale	New scale	
Mass	gr	3.6	4.5	0.8	
Size	mm	18 × 16 × 8	27 × 13 × 8	18 × 13 × 6	
Force	N	7.00	0.20	0.20	
Stroke	mm	± 6	± 3	± 3	
Speed	sec	0.12	0.6	0.6	
Power idle	mA	5	50	50	
Power Avg	mA	30	70	70	
Power max	mA	250	130	130	

with robust enough output still increase the size and mass to such values that the use in MAVs is not yet practical. Moreover, the servo is currently still relatively slow and the piezo drive requires high voltages. The implementation of piezo actuators would require and justify a specific research project on its own.

Table 2.1 summarizes the major specifications of seven different actuators.

## 2.6 Energy and Power

Energy and power are crucial parts of the flapping wing MAV design. The available energy heavily influences the flight time. Power, which is the amount of energy used per second, determines whether flight is possible in the first place. In addition, it is an important factor for determining how maneuverable the MAV is. Both energy and power impact the type of payload that can be carried aboard the MAV. The three characteristics of flight time, maneuverability, and payload capability are essential to

the utility of an MAV's design and often have to be traded off against each other. For instance, if the payload uses more power, then a given energy source might just have enough power to fly but the climb rate might have become ridiculously small. And if more power is used, due to battery characteristics a same battery typically will provide less energy due to higher internal losses. In this section, we will explain some of the main factors influencing the mentioned three characteristics. In Subsection 2.6.1 we discuss flight efficiency and its dependence on the flight regime. Subsequently, in Subsection 2.6.2 we explore different energy storage materials and evaluate their promise and current applicability to light-weight flapping wing MAVs. Afterward, we focus on batteries and explore the trade-off between battery mass and payload mass in Subsection 2.6.3.

### 2.6.1 Flight Efficiency

Micro aircraft are not as efficient as their larger counterparts. At a small size or low velocity the viscosity of the air has a greater influence on the air flow. This low Reynolds number condition generally leads to higher drag and lower lift, implying less efficiency. The efficiency of flight is also related to the way in which the micro aircraft flies. Flapping wing flight exploits the viscous aerodynamic effects and hence partly overcomes the loss of lift. Furthermore, the flight mode of the flapping wing aircraft is of importance. For instance, hovering flight is a quite power intensive flight mode. This is also the case for animals: when hummingbirds hover, they need to feed very often (e.g., every 4–5 min) to stay airborne [16]. Likewise, in hover mode a flapping wing MAV will not be at its most efficient regime and will need more power and will show shorter flight times than at more efficient forward flight speeds.

### 2.6.2 Energy Storage Materials

When considering the qualities of different energy sources we look at the specific energy and specific power of the pure energy storage material. The specific energy measure of highest relevance is the energy-to-weight ratio (kJ/kg), although the energy density (kJ/liter) is also of importance. This also goes for the power-to-weight ratio (kW/kg) and power density (kW/liter). For a choice of energy storage material, we also need to take into account that the energy content of the storage material has to be converted to useable power for the aircraft. The aircraft needs mechanical power for propulsion and electric power for the flight control and payload systems. To convert the potential energy from the source to propulsive and electric power, a conversion system is needed. This conversion system can be simple and efficient for some energy sources while it can be completely impractical for others. The illustrative overview in Table 2.2 is derived from generally available information and can be regarded as representative for the energy carrier but not necessarily absolutely accurate for each application.

**Table 2.2** Different energy sources and their properties

Storage material	Energy type	Energy-to-weight ratio kJ/kg	Power-to-weight ratio kW/kg
Uranium (in breeder)	Nuclear fission	80600000000	
Hydrogen (compressed at 70 MPa)	Chemical	142000	
LPG (including Propane /Butane)	Chemical	46400	
Gasoline (petrol) / Diesel / Fuel oil	Chemical	46000	
Jet fuel	Chemical	43000	
Fat (animal/vegetable)	Chemical	37000	
Coal	Chemical	24000	
Carbohydrates (including sugars)	Chemical	17000	
Protein	Chemical	16800	
Wood	Chemical	16200	
Formic Acid	Chemical	6100	
TNT	Chemical	4600	
Gunpowder	Chemical	3000	
Hydrogenperoxide	Chemical	2600	
Lithium SOCl <sub>2</sub> (primary)	Electrochemical	1800	0.10
Hydrogen Fuel Cell, Medium size, Horizon Aeropack	Electrochemical	2400	0.12
Formic Acid + Fuel Cell System, Small, Neah Power	Electrochemical	1500	0.10
Lithium SOCl <sub>2</sub> (hi-current, primary)	Electrochemical	1140	0.21
Lithium-Sulphur (secondary) (SotA: 2015)	Electrochemical	900	1.13
Lithium-ion -polymer battery	Electrochemical	650	2.80
Small Lithium-polymer battery ( < 0.3 Ah)	Electrochemical	450	2.80
Alkaline battery (primary)	Electrochemical	670	0.06
Nickel-metal hydride battery	Electrochemical	360	0.60
Lead-acid battery	Electrochemical	170	0.10
Supercapacitor	Electrostatic	18	0.50
Electrostatic capacitor	Electrostatic	0.36	30.0

The energy sources in the “chemical” category have very interesting energy densities. For instance, hydrocarbon fuel engines, with internal combustion or jet turbines, are widely used in larger unmanned aircraft. These engines often drive a propeller and an electric generator for electric power to the payload, control and navigation systems. For micro or nano aircraft existing versions of these systems are too large to be accommodated.

Fuel cells that convert the chemical energy to electric power are still novel technology even for the larger unmanned aircraft. These systems are rather complex and only deliver a moderate amount of power, but they can do this for a long time. This restricts the use to efficient long endurance missions in the order of hours. A hybrid power source with a small battery that is constantly topped off can improve the versatility of the fuel cell system. For example, it can be used to deliver a short burst of power during take-off and short climbs. Small commercial systems in this category have a weight of about a kilogram and consequently the minimal mass of the complete UAV with fuel cells will generally not be less than about 2 kg. These systems attain already a very good energy-to-weight ratio, with a power density that is compatible with longer duration flights.

<http://Neahpower.com> is working on a system that uses formic acid as a source of hydrogen that is easier and safer on small scales than pressurized hydrogen. This allows the fabrication of smaller fuel cell systems for smaller UAVs. For MAVs the fuel cell technology is not yet suitable. Although the energy-to-weight ratio of a fuel cell system can be high, their power-to-weight ratio is low, and the high minimum system weight makes them inadequate for the very small MAVs.

There are UAVs flying on prototype Lithium-Sulphur cells made by the company SionPower. The cells have the potential of outperforming the Lithium Polymer battery by a factor of two, but the research progress has been much slower than anticipated. The cells are not yet available commercially but are tested in military and research vehicles like the Qinetiq Zephir. At this stage of development the Li-S cell is 50 % better than the Lithium Polymer in energy-to-weight ratio and a little worse in power-to-weight ratio. In the future this type of battery could be useful when the pace of development proceeds.

The possible use of solid (rocket) fuel has been developed to power small insect like gliders [22]. It could be very interesting for specific types of aircraft, but impractical for the majority of UAV uses due to short burn times.

Promising research takes place on ultra-small catalytic based internal combustion type of actuation for the flapping of the wings. Hydrogenperoxide is injected into a cylinder and is decomposed through the use of a catalyst [36]. This propulsion might be useable in the future for very small, micro or nano flapping wing air vehicles. Electric power for control, navigation and intelligence is still required.

For small to very small aircraft the electric power source in the form of a battery powering an electric motor yields a very interesting compromise between duration and complexity. The energy-to-weight ratio, the power-to-weight ratio and the power density of modern Lithium Polymer batteries is good. Even very small brushless electric motors reach a high power-to-weight ratio of over 1 kW/kg together with a good efficiency and controllability. Therefore, in the following we will limit our discussion to the use of batteries and electric motors.

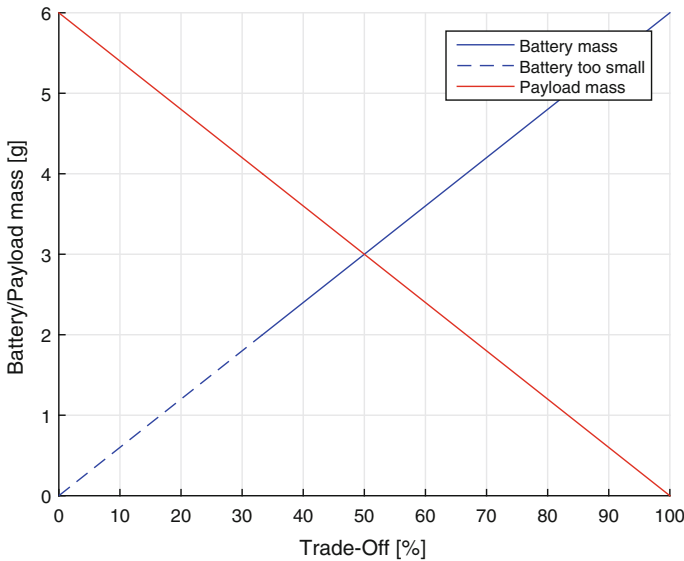


**Fig. 2.7** Battery mass versus payload mass

### 2.6.3 Trading Off Battery Mass and Payload Mass

Given an energy source, a choice has to be made concerning the amount of energy to incorporate into the design. This choice is strongly related to the MAV's envisaged mission and is based on the trade-off between payload, maneuvering capabilities and flight duration. A given aircraft can lift a limited payload mass plus energy source mass with a given amount of maneuverability. Payload mass can be traded off with battery mass as shown in Fig. 2.7. When all the mass is used for energy the duration is maximized at the expense of payload. The minimum mass of the battery is a more complex value and is strongly influenced by the available power. When the energy source becomes small, although it might have sufficient energy for a very short flight, it can not always deliver its energy content sufficiently fast. In other words, the power-to-weight ratio of the battery will typically determine how small a battery can become to still support flight.

It is good to realize that although Fig. 2.7 shows a nice linear trade off in terms of weight, the consequences of choosing a battery and payload mass are not as linear at all. At smaller battery sizes the load factor will significantly increase, which can reduce flight time more than linearly.

Importantly, each battery has its associated (nonlinear) discharge curves (shown for the cyclonE-130 in Fig. 2.8). The discharge curve is determined by the amount of current (A) drawn from the battery. The amount of energy actually used for powering the MAV is represented by the area under each discharge curve ( $V \times \text{mAh}$ ). Relative load is expressed in 'C' and for a 130mAh cell a discharge rate of 1 'C' means

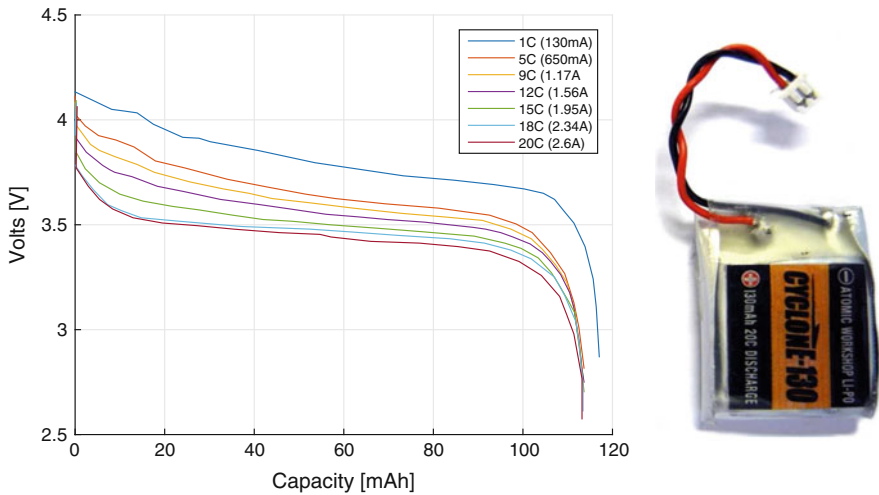


**Fig. 2.8** *Left* Discharge curves of CyclonE-130mAh cell. *Right* CyclonE-130 mA cell with Molex connector [40]

discharging at 130 mA. As can be seen from the plots, the area under the curve gets significantly smaller at higher relative loads.

Figure 2.9 shows the evolution over time of battery voltage at various discharge rates, and the bottom plot illustrates what happens with the lost energy. At higher discharge rates, the temperature rises significantly and further increasing the discharge rate even poses overheating risks.

The efficiency of a battery and also its maximal load depend mainly on the internal resistance of the cells used. Internal resistance is not a clearly-defined and easy-to-measure value but rather a complex chemical process in function of time. It is typically well approximated by measuring the voltage change due to a predefined reproducible load change using Ohm's law.<sup>1</sup> For instance during discharge, the load is dropped completely during 2 seconds and the voltage rise is measured after 2 s of cell relaxation. Figure 2.10 shows the discharge curves of a 150mAh cell and the bottom plot shows how the internal resistance varies during the discharge. A few important things can be noted from this plot. First of all the internal resistance significantly increases when the cell is getting empty. At first sight it might look like higher loads on the battery reduce its internal resistance. In fact it is the higher temperature which is responsible for slightly lower internal resistances. The colder the lithium battery, the higher the internal resistance.

Figure 2.11 computes how much energy the same 150mAh lithium-polymer battery can provide until its voltage drops below a certain voltage threshold. DelFly for instance has a small Electronic Speed Controller (ESC, used for brushless motors)

<sup>1</sup> $I = V/R$ , with  $I$  current,  $V$  voltage, and  $R$  resistance.

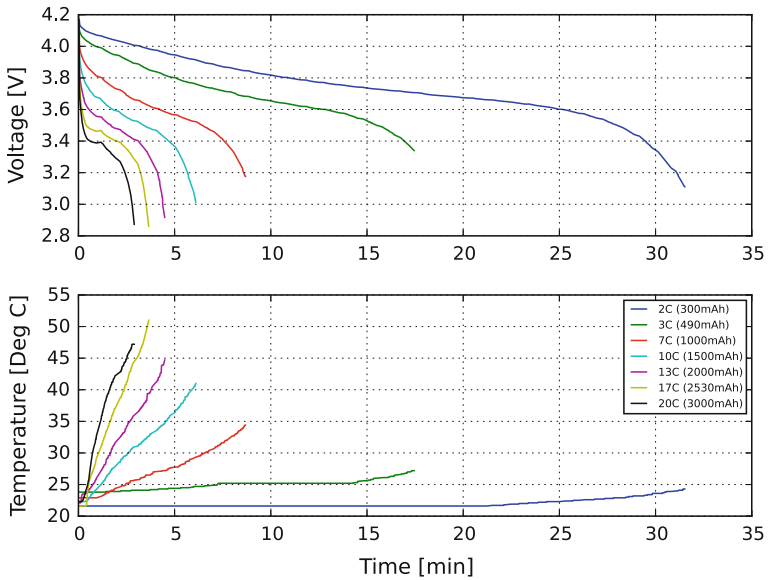


Fig. 2.9 Discharge curves of 150mAh cell

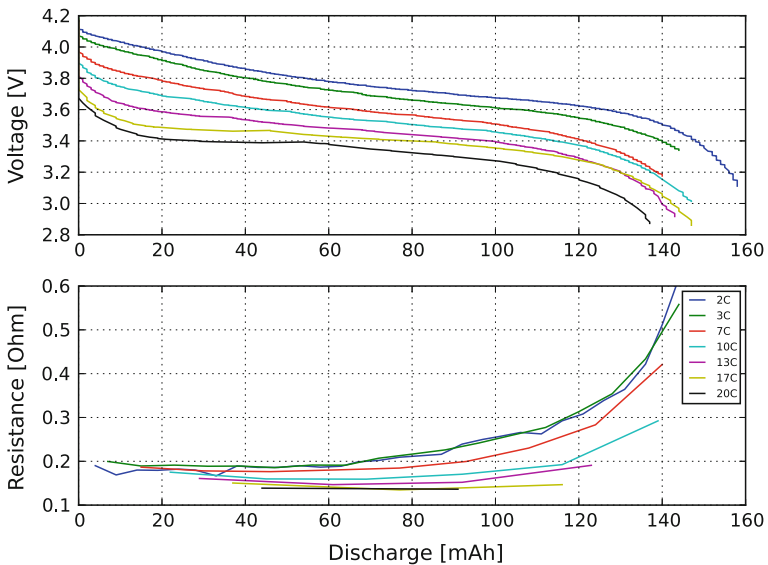
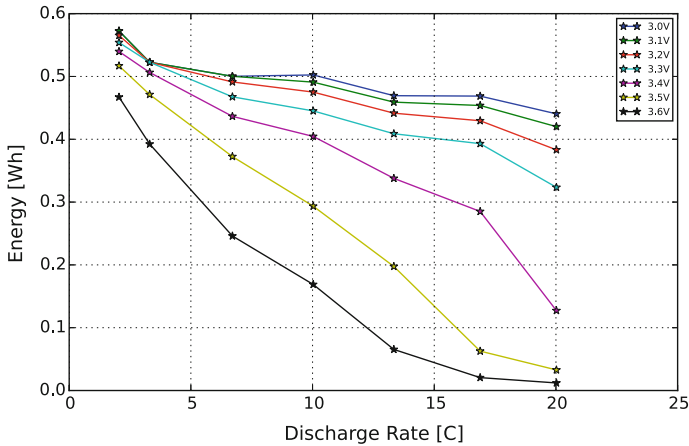


Fig. 2.10 Cell characteristics 150mAh cell

that will function properly down to 3.3 V but not lower. This means that we should only consider the area under the discharge curve for the part in which the voltage is above 3.3 V. The tested cell from Fig. 2.11 would deliver only 0.33Wh until 3.3 V





**Fig. 2.11** Useful energy content 150mAh cell

at 20C compared to 0.55 Wh at 2C, meaning a 40 % reduction in energy content. In other words, if the battery load is 10 times higher, the flight is not 10 times shorter but almost 17 times shorter. Similarly, if for instance an initial battery mass of 6 g is traded for 2 g of additional payload (See Fig. 2.7) resulting in only a 4 g battery, then one might expect  $\frac{1}{3}$  less flight time. However, since the battery is 33 % smaller the relative load of the smaller cell is 50 % higher and so are internal losses. If the low voltage threshold is fixed, the higher load over the battery internal resistance also means the low voltage threshold is reached before the battery is actually empty. Figure 2.11 illustrates that this process can get quite dramatic.

The other way around, when for instance wing efficiency is increased and a lower power is needed, then the lower relative load on the cell will also mean a reduction of losses in the battery, and more useable energy before the low voltage threshold is reached. This is why a 10 % wing efficiency increase can yield more than 10 % extra flying time. This non-linearity is particularly large for very highly loaded or in other words small batteries.

In summary, small changes in mass or efficiency of the propulsion system can have a large impact on the flight duration due to the nonlinear discharge curves and requirements of the electronic components.

## 2.7 Drive and Mechanism

In most small ornithopters the wings oscillate with a frequency of between 8 and 50 Hz, depending on vehicle size and flight regime. To produce this motion one could employ actuators that directly produce a reciprocating movement. A linear or circular electromagnetic actuator like that of the magnetic pick-up head in a hard disk could

be used. The problem is that this will be rather heavy. The actuator has to generate a significant force at a relatively low frequency. As the mass of any electromagnetic system is roughly proportional to the force it can produce, we can see that a high force at a low frequency will result in a heavy actuator.

Electrostatic actuators like those of the piezo type suffer also from a frequency mismatch. These systems perform best at really high frequencies in the order of 50–150 kHz and at low amplitudes. In systems that operate at 8 to 50 Hz the power-to-weight ratio of a piezo actuator is low. The Robobee flies on the basis of a Piezo actuator, flapping at 120 Hz [25]. However, the system currently still needs an external power source, with the power-to-weight ratio inadequate for untethered flight.

A rotational electric motor, also at the scale of micro and nano air vehicles, delivers a good power-to-weight-ratio of around 1 kW/kg at efficiencies of at least 60 % for micro to 40 % for the nano systems. Sensorless, brushless motors are possible at these scales and offer a superior reliability, power-to-weight ratio and efficiency compared to the brushed motors. The control of the sensorless brushless motor is not trivial but the required computing power is low compared to the total system power consumption.

Brushless motors consist of a permanent magnetic component and of a ‘stator’ with electromagnetic coils. The electromagnetic field can be controlled to attract the permanent magnetic components at the right time, making the permanent magnetic component spin around. Two types of brushless motors are known, so called inrunners and outrunners (inset I and II, respectively in Fig. 2.12). With the first type the stator containing the electromagnetic slots is positioned on the outside of the permanent magnetic armature that spins inside of the motor. The outrunner type has a central stator with the electromagnetic slots where the permanent magnetic rotor spins around the stator. The outrunner is preferred in our type of use as it normally produces more torque at a lower rpm (rotations per minute) than the inrunner. The optimal speed range of small outrunners is around 20.000 rpm. This circular

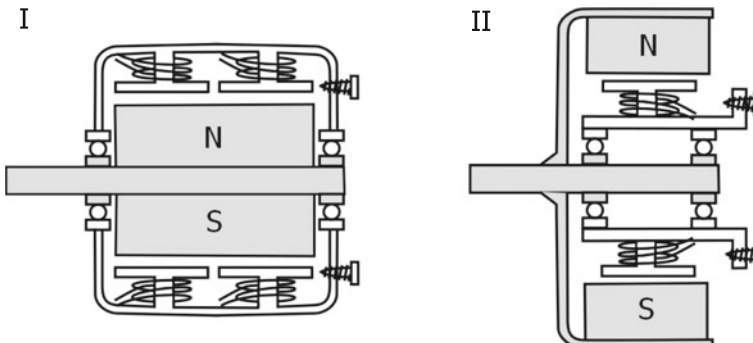


**Fig. 2.12** I: Inrunner brushless motor. II: Outrunner brushless motor. In both cases the magnets are moving (grey) and the coils are static. The inrunner has the magnets at the centre while the outrunner has the magnets around the coils. The inrunner has a static outer case, while the outrunner must be mounted at the stator end, and care must be taken that nothing can touch the rotating outer hull

movement has to be transformed into a reciprocal movement of the right frequency. For instance, the DelFly has a two-stage gearing with a gear ratio of 21.3:1. Therefore, at a motor speed of 19.200 rpm we achieve a representative 15 Hz flapping frequency.

Extreme examples of micro flappers include the extraordinary 1 g ‘Hummer’ [26] (a flapping wing model that served as the basis for the 3 g ‘Da Vinci’ toy), the 2.4 g ‘robot humming bird’ [24], and the 3.07 g DelFly Micro (carrying a camera and transmitter) [7]. At these scales the control of sensorless brushless motors driving highly non-constant aerodynamics loads while the rotational inertia of the motor itself is incredibly small is beyond the reach of current motor controllers. Hence, for such small FWMAVs, brushed motors are unfortunately still the only option.

---

## 2.8 Conclusions

In summary, the general design concept and goal of the flapping wing MAV are the major drivers behind flapping wing design. Subsequently, choices concerning tail and wing configuration largely determine the complexity and capabilities of the design. Just as for the design of larger aircraft, basic choices have to be made regarding the type and mass of the energy source and the payload taken on board. In contrast to larger aircraft, the choices are more restricted due to the small mass. In addition, we have shown that at the scale of small flapping wing MAVs, small changes in mass can have a significant impact on the flight time of the flapping wing MAV.

In the following chapters, we will delve into the specifics of the DelFly design. A major requirement that has been present throughout the project is that the DelFly should be able to perform an observation mission. This requirement has many implications. For instance, a DelFly has to have at least one camera on board. Moreover, a DelFly has to fly for at least a few minutes so that it can fly to a different location at which it needs to perform its observations. In Chap. 3, we discuss the mechanical design choices, including the choice for the X-wing configuration. Subsequently, in Chap. 4, we explain the electronic components on board the DelFly.

---

## References

1. Osaka slow fliers club. <http://blog.goo.ne.jp/flappingwing>
2. S. Avadhanula, R.J. Wood, E. Steltz, J. Yan, R.S. Fearing, Lift force improvements for the micromechanical flying insect, in *IEEE International Conference on Intelligent Robots and Systems*, 28-30 Oct 2003, Las Vegas NV (2003)
3. W. Bejgerowski, A. Ananthanarayanan, D. Mueller, S.K. Gupta, Integrated product and process design for a flapping wing drive-mechanism. *ASME J. Mech. Design* **131** (2009)
4. O. Chanute, *Progress in Flying Machines* (Dover, 1894, reprinted 1998)
5. Toki Corporation. <http://www.toki.co.jp/>

6. DARPA, The nano hummingbird surveillance and reconnaissance aircraft developed by aerovironment, inc. under contract to the united states government's defense advanced research projects agency. [http://commons.wikimedia.org/wiki/File:Nano\\_Hummingbird.jpg](http://commons.wikimedia.org/wiki/File:Nano_Hummingbird.jpg) (2011)
7. G.C.H.E. de Croon, K.M.E. de Clercq, R. Ruijsink, B. Remes, C. de Wagter, Design, aerodynamics, and vision-based control of the delfly. *Int. J. Micro Air Veh.* **1**(2), 71–97 (2009)
8. G.C.H.E. de Croon, M.A. Groen, C. De Wagter, B.D.W. Remes, R. Ruijsink, B.W. van Oudheusden, Design, aerodynamics, and autonomy of the delfly. *Bioinspir. Biomimet.* **7**(2) (2012)
9. X. Deng, L. Schenato, S.S. Sastry, Flapping flight for biomimetic robotic insects: part ii-flight control design. *IEEE Trans. Robot.* **22**(4), 789–803 (2006)
10. X. Deng, L. Schenato, W.C. Wu, S.S. Sastry, Flapping flight for biomimetic robotic insects: part i-system modeling. *IEEE Trans. Robot.* **22**(4), 776–788 (2006)
11. R.S. Fearing, K.H. Chiang, M. Dickinson, D.L. Pick, M. Sitti, J. Yan, Wing transmission for a micromechanical flying insect, in *IEEE International Conference on Robotics and Automation, April, 2000* (2000)
12. S.B. Fuller, M. Karpelson, A. Censi, K.Y. Ma, R.J. Wood, Controlling free flight of a robotic fly using an onboard vision sensor inspired by insect ocelli. *J. R. Soc. Interface* **11**(97) (2014)
13. N. Gaissert, R. Mugrauer, G. Mugrauer, A. Jebens, K. Jebens, E.M. Knubben, Inventing a micro aerial vehicle inspired by the mechanics of dragonfly flight, in *Towards Autonomous Robotic Systems*, pp. 90–100. Springer (2014)
14. J. Gerdes, A. Holness, A. Perez-Rosado, L. Roberts, A. Greisinger, E. Barnett, J. Kempny, D. Lingam, C.-H. Yeh, A. Bruck Hugh et al., Robo raven: a flapping-wing air vehicle with highly compliant and independently controlled wings. *Soft Robot.* **1**(4), 275–288 (2014)
15. J.W. Gerdes, S.K. Gupta, S. Wilkerson, A review of bird-inspired flapping wing miniature air vehicle designs. *J. Mech. Robot.* **4**(2) (2012)
16. R. Hainsworth, L. Wolf, Hummingbird feeding. *Wildbird Magazine* (1993)
17. C.-K. Hsu, J. Evans, S. Vytla, P.G. Huang, Development of flapping wing micro air vehicles - design, CFD, experiment and actual flight, in *48th AIAA Aerospace Sciences Meeting Including the New Horizons Forum and Aerospace Exposition, Orlando, Florida* (2010)
18. M. Karasek, A. Hua, Y. Nan, M. Lalami, A. Preumont, Pitch and roll control mechanism for a hovering flapping wing MAV, in *IMAV 2014: International Micro Air Vehicle Conference and Competition 2014*, Delft, The Netherlands, 12–15 Aug 2014
19. M. Karásek, A. Preumont, Flapping flight stability in hover: a comparison of various aerodynamic models. *Int. J. Micro Air Veh.* **4**(3), 203–226 (2012)
20. M. Keennon, K. Klingebiel, H. Won, A. Andriukov, Development of the nano hummingbird: a tailless flapping wing micro air vehicle, in *50th AIAA Aerospace Science Meeting*, pp. 6–12 (2012)
21. Hobby King. <http://www.hobbyking.com/>
22. M. Kovac, M. Bendana, R. Krishnan, J. Burton, M. Smith, R.J. Wood, Multi-stage micro rockets for robotic butterflies. *Robot. Syst. Sci.* (2012)
23. N. Leichty, Micro flier radio. <http://microflierradio.com/>
24. H. Liu, X. Wang, T. Nakata, K. Yoshida, Aerodynamics and flight stability of a prototype flapping Micro Air Vehicle, in *2012 ICME International Conference on Complex Medical Engineering (CME)*, pp. 657–662 (2012)
25. K.Y. Ma, P. Chirarattananon, S.B. Fuller, R.J. Wood, Controlled flight of a biologically inspired, insect-scale robot. *Science* **340**(6132), 603–607 (2013)
26. P. Muren, The 'hummer', a 1-gram flapping wing micro air vehicle, presented at EMAV 2007 (2007)
27. Plantraco. <http://www.plantraco.com/>
28. T.N. Pornsin-Sirirak, Y.-C. Tai, C.-M. Ho, M. Keennon, Microbat: A palm-sized electrically powered ornithopter, in *NASA/JPL Workshop on Biomimetic Robots*, Pasadena, USA (2001)
29. C. Richter, H. Lipson, Untethered hovering flight of a 3d-printed mechanical insect. *Artif. Life* **17**, 73–86 (2011)

30. P.C.S. Fuller, E. Helbling, R. Wood, Using a gyroscope to stabilize the attitude of a fly-sized hovering robot, in *International Micro Air Vehicle Competition and Conference 2014*, pp. 102–109, Delft, The Netherlands (August 2014)
31. E. Steltz, S. Avadhanula, R.S. Fearing, High lift force with 275 hz wing beat in MFI, in *IEEE International Conference on Intelligent Robots and Systems* (2007)
32. E. Steltz, R.S. Fearing, Dynamometer power output measurements of piezoelectric actuators, in *IEEE International Conference on Intelligent Robots and Systems* (2007)
33. M. Sun, Y. Xiong, Dynamic flight stability of a hovering bumblebee. *J. Exp. Biol.* **208**(3), 447–459 (2005)
34. G.K. Taylor, L.R.T. Adrian, Dynamic flight stability in the desert locust *schistocerca gregaria*. *J. Exp. Biol.* **206**(16), 2803–2829 (2003)
35. New Scale Technologies. <http://www.newscaletech.com/>
36. T. van Wageningen, Design analysis for a small scale hydrogen peroxide powered engine for a flapping wing mechanism micro air vehicle. Master's thesis, Delft University of Technology (2012)
37. C. De Wagter, The delfly micro ia a 10 cm wing span 3.07 grams flapping wing mav equipped with a camera. it was first built in 2008. [https://en.wikipedia.org/wiki/DelFly#/media/File:DelFly\\_Micro\\_2008\\_V1.jpg](https://en.wikipedia.org/wiki/DelFly#/media/File:DelFly_Micro_2008_V1.jpg) (2008)
38. R.J. Wood, The first takeoff of a biologically-inspired at-scale robotic insect. *IEEE Trans. Robot.* **24**(2), 341–347 (2008)
39. R.J. Wood, S. Avadhanula, R.S. Fearing, microrobotics using composite materials: the micro-mechanical flying insect thorax, in *IEEE International Conference on Robotics and Automation 2003, Taipei, Taiwan*, pp. 1842–1849 (2003)
40. Atomic Workshop. <http://www.atomicworkshop.co.uk/>
41. P. Zdunich, D. Bilyk, M. MacMaster, D. Loewen, J. DeLaurier, R. Kornbluh, T. Low, S. Stanford, D. Holeman, Development and testing of the mentor flapping-wing micro air vehicle. *J. Aircr.* **44**(5), 1701–1711 (2007)

<http://www.springer.com/978-94-017-9207-3>

The DelFly

Design, Aerodynamics, and Artificial Intelligence of a  
Flapping Wing Robot

de Croon, G.C.H.E.; Perçin, M.; Remes, B.D.W.; Ruijsink,  
R.; De Wagter, C.

2016, XIV, 218 p. 124 illus., 11 illus. in color., Hardcover

ISBN: 978-94-017-9207-3